

L. ZSCHIEDRICH, R. KLOSE, A. SCHÄDLE, F. SCHMIDT

**A new Finite Element realization of the
Perfectly Matched Layer Method for
Helmholtz scattering problems on
polygonal domains in 2D**

A new Finite Element realization of the Perfectly Matched Layer Method for Helmholtz scattering problems on polygonal domains in 2D

L. Zschiedrich, R. Klose, A. Schädle, F. Schmidt

Konrad-Zuse-Zentrum Berlin, Takustr. 7, D-14195 Berlin-Dahlem.

Abstract

In this paper we propose a new finite element realization of the Perfectly Matched Layer method (PML-method). Our approach allows to deal with arbitrary shaped polygonal domains and with certain types of inhomogeneous exterior domains. Among the covered inhomogeneities are open waveguide structures playing an essential role in integrated optics. We give a detailed insight into implementation aspects. Numerical examples show exponential convergence behavior to the exact solution with the thickness of the PML sponge layer.

Key words: transparent boundary conditions, perfectly matched layer, pole condition

1 Introduction

Scattering problems arising from integrated optics are modeled by Maxwell's equations on unbounded domains. Typically waveguide structures connect various sub-components over a distance of a large number of wavelengths. A central task in the numerical solution of such problems is the implementation of transparent boundary conditions, which is often realized by Berenger's Perfectly Matched Layer method (PML-method) [1,3,4,2]. Monk and Collino [5] introduce the PML-method in a homogeneous medium for separable coordinate systems as a complex continuation in one distance variable by exploiting the analyticity of the solution. For this case Lassas et al. prove the exponential convergence of the PML-method [10]. By introducing a normal tangential coordinate system they extend these results to general convex domains [11]. This coordinate system is defined by a parametrization of the boundary (τ variable)

and the Euclidian distance ν from the boundary, cf. Fig. 1. Their proof for the convergence of the PML-method in a homogeneous medium is based on a complex continuation in ν -direction. However in typical applications from integrated optics, see Figs. 1, 3, the solution may only be analytic in a direction different from ν . In Fig. 1 the scatched waveguide cuts the τ -isolines. Hence the solution is not analytic in ν -direction.

In this paper we propose a new realization of the PML-method by introducing coordinate systems which we call prismatoidal. This yields a clear concept on a semi-discrete level. Our approach allows a flexible adaption to many geometries, even with inhomogeneous exterior domains, cf. Fig. 2. In contrast to [9] the definition of a complex Riemann metric on a continuous level is avoided. We restrict ourselves to the two dimensional case for the sake of a clear presentation of the underlying concept. The ideas carry over to the three dimensional case and to the vectorial Maxwell equations [13] as we will present in a future paper.

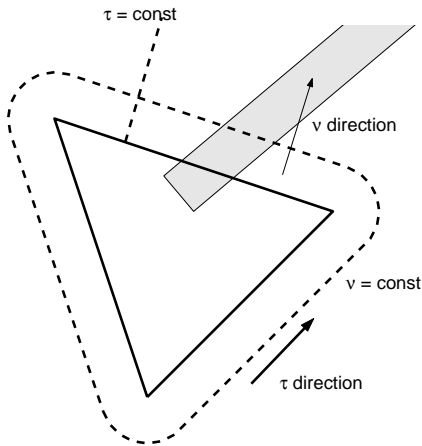


Fig. 1. Normal-tangential coordinate system used by Lassas et. al. The waveguide structure yields solutions not analytic in ν -direction.

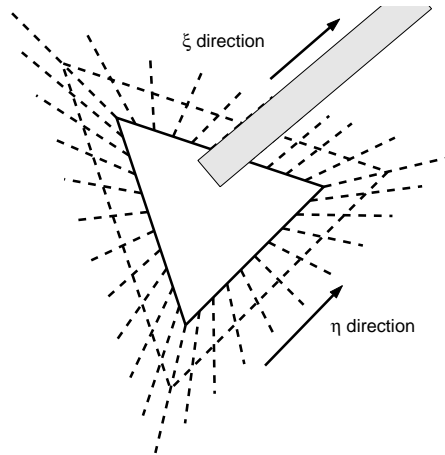


Fig. 2. Prismatoidal coordinate system. The waveguide structure yields solutions analytic in ξ -direction.

Maxwell's time harmonic equations for a source and current free medium lead to the photonic wave equations. We consider the two dimensional case. For TE-polarization the H-field takes the form $(0, 0, H_z)$, and the first photonic wave equation reads

$$\nabla \cdot \left(\frac{1}{\epsilon(x, y)} \nabla H_z(x, y) \right) + \frac{\omega^2}{c^2} H_z(x, y) = 0. \quad (1)$$

For TM-polarization the E-field takes the form $(0, 0, E_z)$, and the second pho-

tonic wave equation reads

$$\Delta E_z(x, y) + \frac{\omega^2}{c^2} \epsilon(x, y) E_z(x, y) = 0. \quad (2)$$

In the sequel we deal with the case of TM-polarization. The unbounded domain is divided into an inner domain Ω and an exterior domain Ω_{ext} . On the common boundary of the interior and the exterior domain, the field u separates into a given incoming field u_i and a scattered field u_s . The scattering problem is determined by

$$\Delta u(\mathbf{x}) + k^2(\mathbf{x})u(\mathbf{x}) = 0 \quad \text{in } \Omega, \quad (3)$$

$$\Delta u_s(\mathbf{x}) + k^2(\mathbf{x})u_s(\mathbf{x}) = 0 \quad \text{in } \Omega_{ext}, \quad (4)$$

$$u(\mathbf{x}) = u_i(\mathbf{x}) + u_s(\mathbf{x}) \quad \text{on } \partial\Omega, \quad (5)$$

$$\partial_\xi u(\mathbf{x}) = \partial_\xi u_i(\mathbf{x}) + \partial_\xi u_s(\mathbf{x}) \quad \text{on } \partial\Omega. \quad (6)$$

Here ξ denotes the non-tangential coordinate of the prismatoidal coordinate system described in Section 2. The scattered field has to satisfy a radiation condition at infinity. For homogeneous exterior domains this is the Sommerfeld radiation condition [8],

$$\lim_{r \rightarrow \infty} r^{\frac{d-1}{2}} \left(\frac{\partial u}{\partial r} - iku \right) = 0. \quad (7)$$

For $d > 1$ this implies that the field decays uniformly for all directions $\hat{x} = x/\|x\|$. Further the field is an outgoing monochromatic wave. For inhomogeneous exterior domains the Sommerfeld radiation condition does not hold true. For example regard an exterior domain such as depicted in Fig. 3. Two straight waveguides with local wavenumbers k_{wg1} and k_{wg2} range from the interior domain to infinity. Such structures guide eigenmodes without damping in the direction of the waveguides. These types of solutions do not exist for homogeneous equations, since the Sommerfeld radiation condition implies the decay of the fields. Furthermore a waveguide may support a couple of eigenmodes with different propagation constants. Therefore the field is asymptotically not monochromatic. F. Schmidt proposes a general concept called pole condition to define radiation conditions for scattering problems [12]. In [6] it is shown that the pole condition is equivalent to the Sommerfeld radiation condition for homogeneous exterior domains. The pole condition leads to new algorithms to construct transparent boundary conditions [12]. Further it gives a new insight to PML. In [7] Hohage et al. prove the convergence of the PML-method for separable but inhomogeneous exterior domains. The aim of this paper is to propose a new finite element realization of the PML-method which is based on the theoretical concepts given in [12]. We do not aim to prove existence and uniqueness of the sought solutions. However various numerical examples indicate experimental convergence of the method.

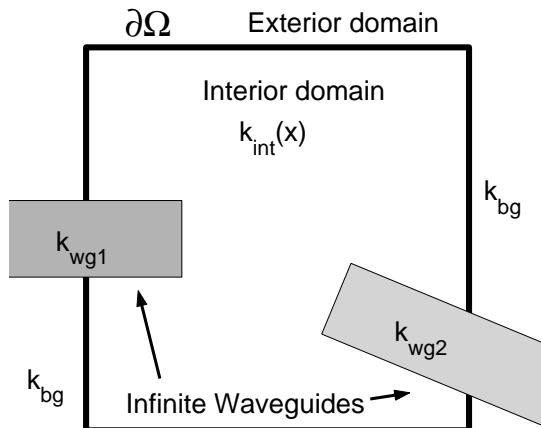


Fig. 3.

2 Local prismatoidal coordinate systems in two dimensions

This section summarizes geometrical aspects of the pole condition approach [12], which are the basis for the proposed realization of the PML method. The central idea is to decompose the exterior domain into a finite number of segments and to associate with each segment a local coordinate system, such that a global distance variable ξ can be introduced. We realize the PML-method as a complex continuation along the ξ - direction. This is analogue to the approach by Collino and Monk [5] for global separable coordinate systems. Our approach resembles the definition of a global normal-tangential coordinate system in [11]. We stress the flexibility and the easy way of implementation of the method in the finite element context. The decomposition of the exterior

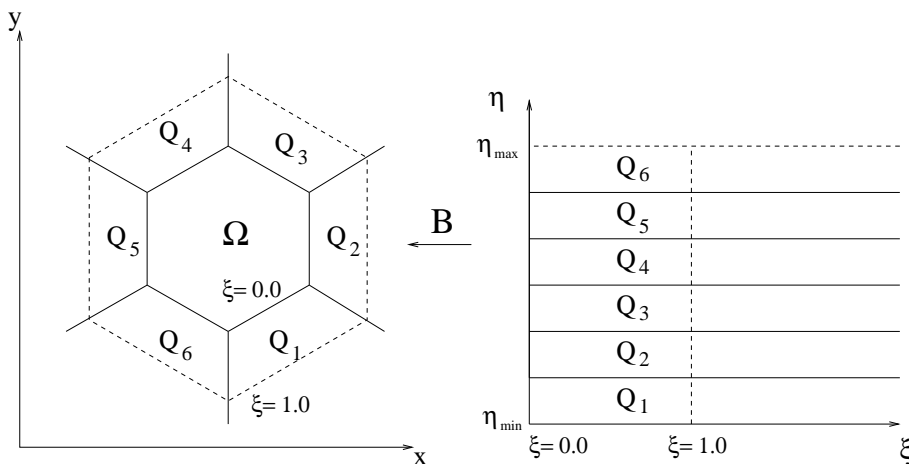


Fig. 4. Prismatoidal coordinate system. Each segment Q_j is the image of a reference element under a bilinear mapping B_j^{loc} . These local mappings are combined to a global mapping B which is continuous in η .

domain into a finite number of segments is based on straight non-intersecting

rays \mathbf{g}_j , which connect each vertex \mathbf{p}_j ($j = 1, \dots, N$) of the polygonal boundary $\partial\Omega$ with infinity. The set of rays together with the boundary $\partial\Omega$ generate a decomposition $\mathcal{L} = \{Q_1, \dots, Q_N\}$ of $\overline{\Omega_{ext}}$. The constructed segments Q_j must be convex semi-infinite quadrilaterals.

We define a relation between the $\xi\eta$ -coordinate system of a reference rectangle and the xy -coordinate system of each rectangle Q_j (e.g. Fig. 4). For each Q_j we construct a bilinear transformation

$$B_j^{loc} : Q_j^{(\xi,\eta)} \rightarrow Q_j^{(x,y)} \quad (8)$$

from the semi-infinite reference rectangle $Q_{ref} := [0, \infty] \times [0, 1]$ onto Q_j , such that the images of two lines $\xi_1 \times [0, 1] \in Q_{ref}$ and $\xi_2 \times [0, 1] \in Q_{ref}$ remain parallel under B_j^{loc} . This is possible due to the convexity of $Q_j^{(x,y)}$. In the following we define a prismatoidal coordinate system, whereas the name is chosen in accordance with a future definition in three dimensions.

Definition 1 (Prismatoidal coordinate system) *Let Ω be a convex domain with polygonal boundary. Each vertex \mathbf{p}_j of $\partial\Omega$ is connected with a straight ray \mathbf{g}_j , such that the set of rays is non-intersecting and a decomposition of Ω_{ext} into a finite number of convex semi-infinite segments Q_j is generated. The local bilinear mappings B_j^{loc} (8) associated with the segments Q_j are combined to a global transformation*

$$B : \overline{\Omega_{ext}^{(\xi,\eta)}} \rightarrow \overline{\Omega_{ext}^{(x,y)}}, \quad (9)$$

such that B is continuous and periodic in η . The Jacobian of B is denoted by J .

Note that B is linear in ξ for fixed η . We give two different ways to construct prismatoidal coordinate systems [12].

Example 2 (Radial Rays) *Let a nonempty convex domain be given. Connect a fixed arbitrary interior point by line segments with each of the vertices of the boundary. Extend these line segments to linear rays, cf. Fig. 5. For a star-shaped non-convex domain there exists an interior point such that any line segment which connects this point with a vertex of the boundary hits the boundary only at this vertex. The line segments defined this way lead to a prismatoidal coordinate system, cf. Fig. 6.*

Example 3 (Generalized normal rays) *Let a nonempty convex domain be given. Construct the rays successively corresponding to all but the last marked vertex such that the rays \mathbf{g}_j have a representation $\mathbf{g}_j(\tau) = \mathbf{p}_j + \tau(c_i\mathbf{e}_i + c_k\mathbf{e}_k)$ with $\tau \in \mathbb{R}_+$ and both c_i, c_k strictly negative. The unit vectors \mathbf{e}_i and \mathbf{e}_k are given by $\mathbf{e}_i = (\mathbf{p}_i - \mathbf{p}_j)/|\mathbf{p}_i - \mathbf{p}_j|$ and $\mathbf{e}_k = (\mathbf{p}_k - \mathbf{p}_j)/|\mathbf{p}_k - \mathbf{p}_j|$, in which \mathbf{p}_i and \mathbf{p}_k are the neighboring nodes to \mathbf{p}_j on the boundary. The last ray is constructed*

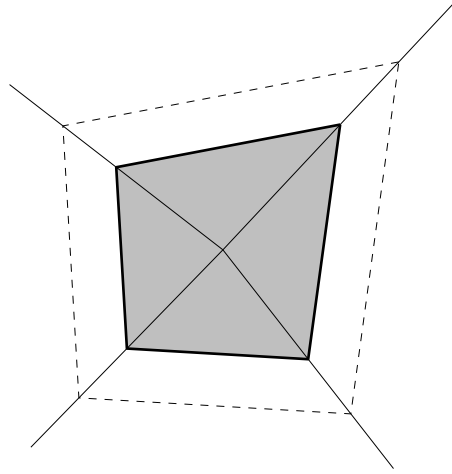


Fig. 5. Radial ray construction for convex domains

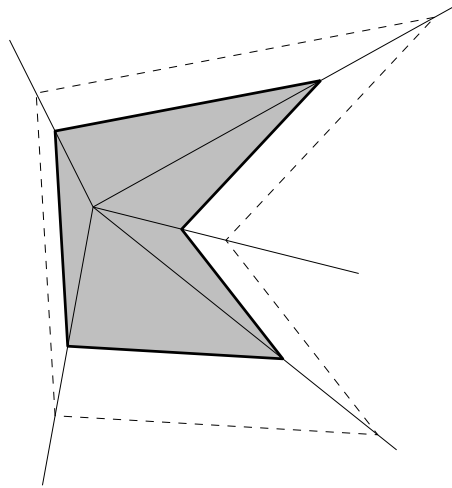


Fig. 6. Radial ray construction for star-shaped concave domain

according to the following scheme:

- (1) Fix an arbitrary point on the ray through the first marked vertex.
- (2) Construct the two lines which go through this point, and which are parallel to their corresponding boundary segments.
- (3) Move in positive direction and continue the following procedure: Determine the intersection point between the parallel line to the boundary and the next ray. Then construct a line through this point, parallel to the next boundary segment.
- (4) The last ray must be constructed such that it goes through the last marked vertex and the intersection of the first and the last line constructed this way.

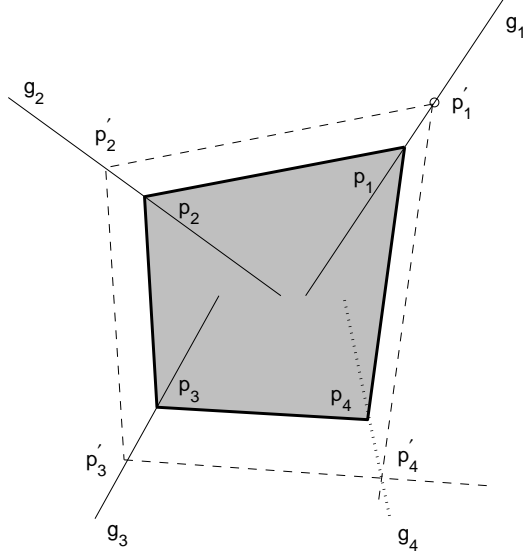


Fig. 7. Generalized normal ray construction for convex domains.

3 PML-method based on local prismatoidal coordinate systems

In this section we introduce a new realization of the PML-method, based on the local prismatoidal coordinate systems from Section 2. Our approach relies on a finite element solution of the scattering problem (3)-(6).

The discrete form of the weak interior problem reads: Seek $u^h \in V_h \subset H^1(\Omega)$ such that for all $v^h \in V_h$

$$\int_{\Omega} \nabla u^h(\mathbf{x}) \cdot \nabla v^h(\mathbf{x}) dx - \int_{\Omega} k^2(\mathbf{x}) u^h(\mathbf{x}) v^h(\mathbf{x}) dx = \int_{\partial\Omega} \partial_n u^h(\mathbf{x}) v^h(\mathbf{x}) ds. \quad (10)$$

The exterior problem can be formulated in the ξ, η -coordinate-system. The transformed Helmholtz-equation is given by

$$\nabla_{\xi, \eta} \cdot (J^{-1} J^{-T} |J| \nabla_{\xi, \eta}) u_s + |J| k^2 u_s = 0. \quad (11)$$

We assume a segment-wise constant wave number k . This ensures analyticity of the scattered field u_s in ξ -direction which is a necessary condition for an application of the PML-method [10]. Nevertheless enough flexibility is left for the configuration of the exterior domain by a proper choice of the segments.

With $F := J^{-1}J^{-T}|J|$ and

$$\begin{aligned} a_2(v, \partial_{\xi\xi}u_s) &= \int_{\Gamma_\eta} v F_{11} \partial_{\xi\xi} u_s d\eta, \\ a_1(v, \partial_\xi u_s) &= \int_{\partial_\eta} v \partial_\xi F_{11} \partial_\xi u_s d\eta - \int_{\Gamma_\eta} (\partial_\eta(v F_{12}) + (\partial_\eta v) F_{21}) \partial_\xi u_s d\eta, \\ a_0(v, u_s) &= \int_{\Gamma_\eta} v \partial_\xi F_{12} \partial_\eta u_s d\eta - \int_{\Gamma_\eta} \partial_\eta v F_{22} \partial_\eta u_s d\eta + \int_{\Gamma_\eta} v |J| k^2 u_s d\eta, \end{aligned}$$

the variational form of the exterior problem reads: Find $u_s \in W^2(\Omega_{ext}^{(\xi,\eta)})$ such that for all $v \in H_\pi^1(\eta_{min}, \eta_{max})$ and all $\xi \in \mathbb{R}_+$

$$a_0(v, u_s) + a_1(v, \partial_\xi u_s) + a_2(v, \partial_{\xi\xi}^2 u_s) = 0, \quad (12)$$

$$u_s(0, \eta) = u_D(\eta), \quad (13)$$

$$\partial_\xi u_s(0, \eta) = u_N(\eta). \quad (14)$$

Here $H_\pi^1(\eta_{min}, \eta_{max})$ is the space $H^1([\eta_{min}, \eta_{max}])$ with periodic functions. The function space $W^2(\Omega_{ext}^{(\xi,\eta)})$ is defined as

$$W^2(\Omega_{ext}^{(\xi,\eta)}) = \begin{cases} w(\xi_0, \eta) \in H_\pi^1(\eta_{min}, \eta_{max}) : \xi_0 \in \mathbb{R}, \text{ fixed}, \\ w(\xi, \eta_0) \in C^2(\mathbb{R}_+) : \eta_0 \in [\eta_{min}, \eta_{max}], \text{ fixed}. \end{cases}$$

The coupling between interior and exterior problem is determined by (13) and (14). Instead of introducing the PML-layer in the continuous variational formulation (12), we perform a discretization in η and realize the PML-method as a complex continuation on a semi-discrete level.

The field component u_s is approximated by

$$u_s^h(\xi, \eta) = \sum_{j=1}^{N_B} u_{s,j}^h(\xi) \psi_j(\eta), \quad (15)$$

where $\{\psi_1, \dots, \psi_{N_B}\}$ is a basis of $S_h \subset H_\pi^1(\eta_{min}, \eta_{max})$. The space S_h is the trace space of the finite element space V_h of the interior problem. The coefficient-vector of $u_s^h(\xi, \eta)$ is denoted by $\mathbf{u}_s^h(\xi)$. Inserting (15) in (12) for u_s yields the system

$$A_0(\xi) \mathbf{u}_s^h(\xi) + A_1(\xi) \partial_\xi \mathbf{u}_s^h(\xi) + A_2(\xi) \partial_\xi^2 \mathbf{u}_s^h(\xi) = 0. \quad (16)$$

The matrices $A_0(z), A_1(z), A_2(z)$, $z \in \mathbb{C}$, are analytic for $\Re(z) > 0$, as we show in Section 4. Therefore a solution of (16) has a complex continuation [14]. Motivated by the case of a homogeneous exterior domain we expect an exponential damping of the solution for $\Im(z) \rightarrow +\infty$. The PML-method is realized by replacing the variable ξ in (16) with the complex extension $\bar{\xi} = \gamma\xi$

and by replacing the unbounded domain Ω_{ext} with the bounded domain Ω_{PML} .
With

$$\gamma = 1 + i\sigma \quad \text{and} \quad \mathbf{u}_{\text{PML}}(\xi) := \mathbf{u}_s(\gamma\xi), \quad (17)$$

the PML system is determined by

$$A_0(\gamma\xi)\mathbf{u}_{\text{PML}}(\xi) + A_1(\gamma\xi)\frac{1}{\gamma}\partial_\xi\mathbf{u}_{\text{PML}}(\xi) + A_2(\gamma\xi)\frac{1}{\gamma^2}\partial_\xi^2\mathbf{u}_{\text{PML}}(\xi) = 0. \quad (18)$$

Remark 4 *The formulation of the exterior problem in local prismatoidal coordinate systems also builds up the basis for other realizations of transparent boundary conditions. In [12] (16) is the starting point for the implementation of the pole condition.*

4 Computation of local matrices in the semi-discrete exterior system

We compute local contributions to the matrices A_0, A_1, A_2 in (16) for the simple case of linear C^0 -elements. The generalization to higher order elements is straightforward.

The system matrices A_0, A_1 and A_2 from (16) are given by

$$\begin{aligned} A_{2,ij}\partial_{\xi\xi}u_{s,j}^h &:= a_2(\psi_i, \psi_j)\partial_{\xi\xi}u_{s,j}^h = \left(\int_{\Gamma_\eta} \psi_i F_{11} \psi_j d\eta \right) \partial_{\xi\xi}u_{s,j}^h, \\ A_{1,ij}\partial_\xi u_{s,j}^h &:= a_1(\psi_i, \psi_j \partial_\xi u_{s,j}^h) \\ &= \left(\int_{\Gamma_\eta} \psi_i (\partial_\xi F_{11} \psi_j + F_{12} \partial_\eta \psi_j) d\eta - \int_{\Gamma_\eta} \partial_\eta \psi_i F_{21} \psi_j d\eta \right) \partial_\xi u_{s,j}^h, \\ A_{0,ij}u_{s,j}^h &:= a_0(\psi_i, \psi_j u_{s,j}^h) \\ &= \left(\int_{\Gamma_\eta} (\psi_i \partial_\eta \psi_j \partial_\xi F_{12} - \partial_\eta \psi_i \partial_\eta \psi_j F_{22} + |J|k^2 \psi_i \psi_j) d\eta \right) u_{s,j}^h. \end{aligned}$$

On the unit segment $[0, 1]$ basis functions are given by

$$\tilde{v}_1(\eta) = 1 - \eta \quad \tilde{v}_2(\eta) = \eta. \quad (19)$$

Local contributions from a segment k are

$$\begin{aligned} (A_2^{(k)})_{ij} &= h \int_0^1 \tilde{v}_i \tilde{v}_j F_{11} d\eta, \\ (A_1^{(k)})_{ij} &= h \int_0^1 (\tilde{v}_i \tilde{v}_j \partial_\xi F_{11} + \frac{1}{h} \tilde{v}_i \partial_\eta \tilde{v}_j F_{12} - \frac{1}{\partial_\eta} \tilde{v}_i \tilde{v}_j F_{21}) d\eta, \\ (A_0^{(k)})_{ij} &= h \int_0^1 (\frac{1}{h} \tilde{v}_i \partial_\eta \tilde{v}_j \partial_\xi F_{12} - \frac{1}{h^2} \partial_\eta \tilde{v}_i \partial_\eta \tilde{v}_j F_{22} + \tilde{v}_i \tilde{v}_j |J|k^2) d\eta, \end{aligned} \quad (20)$$

for $i, j \in \{1, 2\}$. To compute these matrices it is necessary to derive the transformations $B_j^{loc} : Q_j^{(\xi, \eta)} \rightarrow Q_j^{(x, y)}$.

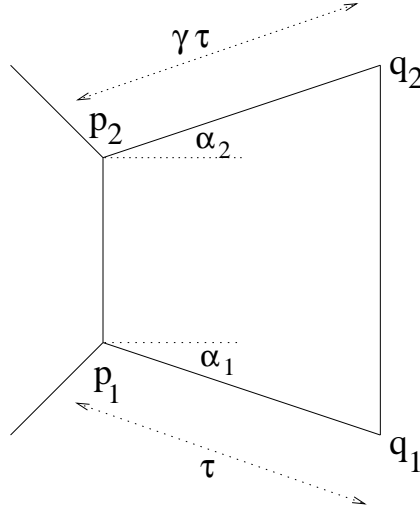


Fig. 8. Segment $Q_j^{(x, y)}$.

Segment j (Fig. 8) is bounded by two rays through the points $p_1 q_1$ respectively $p_2 q_2$, with parameter representations

$$\begin{aligned} \mathbf{g}_1(\tau) &= \mathbf{p}_1 + \tau \mathbf{e}_1 \\ \mathbf{g}_2(\tau) &= \mathbf{p}_2 + \gamma \tau \mathbf{e}_2 \end{aligned} \quad (21)$$

where $\mathbf{e}_1, \mathbf{e}_2$ are the unit vectors

$$\begin{aligned} \mathbf{e}_1 &= (\mathbf{q}_1 - \mathbf{p}_1) / (|\mathbf{q}_1 - \mathbf{p}_1|) \\ \mathbf{e}_2 &= (\mathbf{q}_2 - \mathbf{p}_2) / (|\mathbf{q}_2 - \mathbf{p}_2|). \end{aligned} \quad (22)$$

and γ is a scaling factor. Since we require $\overline{p_1 p_2} \parallel \overline{q_1 q_2}$, it holds

$$\gamma \tau \cos \alpha_2 = \tau \cos \alpha_1 \Rightarrow \gamma = \frac{\cos \alpha_1}{\cos \alpha_2}. \quad (23)$$

We define ξ as the distance between the line through p_1 and p_2 and the line through q_1 and q_2 , $\xi := \tau \cos \alpha_1$. This yields a symmetric parameter representation for the rays,

$$\begin{aligned} \mathbf{g}_1(\xi) &= \mathbf{p}_1 + \frac{\xi}{\zeta \cos \alpha_1} \mathbf{e}_1 \\ \mathbf{g}_2(\xi) &= \mathbf{p}_2 + \frac{\xi}{\zeta \cos \alpha_2} \mathbf{e}_2. \end{aligned} \quad (24)$$

with $\xi \geq 0$ and a scaling factor ζ that may vary from segment to segment. If ζ and α_1 correspond to an arbitrary segment and ζ_p and $\alpha_{2,p}$ to the previous segment,

$$\zeta = (\zeta_p \cos \alpha_{2,p}) / \cos \alpha_1 \quad (25)$$

ensures that these two segments fit continuously. The transformation between the $\xi\eta$ - and the xy -coordinate-system is

$$\begin{pmatrix} x \\ y \end{pmatrix} = \mathbf{g}_1(\xi) + \frac{\eta - \eta_1}{\eta_2 - \eta_1} (\mathbf{g}_2(\xi) - \mathbf{g}_1(\xi)). \quad (26)$$

With $\mathbf{e}_1 = (\cos \beta_1, \sin \beta_1)$ and $\mathbf{e}_2 = (\cos \beta_2, \sin \beta_2)$ the mapping B_j^{loc} is given by

$$\begin{aligned} \begin{pmatrix} x \\ y \end{pmatrix} &=: B_j^{loc}(\xi, \eta) \\ &= \left(1 - \frac{\eta - \eta_1}{\eta_2 - \eta_1}\right) \begin{pmatrix} x_1 \\ y_1 \end{pmatrix} + \frac{\xi}{\zeta \cos \alpha_1} \begin{pmatrix} \cos \beta_1 \\ \sin \beta_1 \end{pmatrix} \\ &\quad + \frac{\eta - \eta_1}{\eta_2 - \eta_1} \begin{pmatrix} x_2 \\ y_2 \end{pmatrix} + \frac{\xi}{\zeta \cos \alpha_2} \begin{pmatrix} \cos \beta_2 \\ \sin \beta_2 \end{pmatrix}. \end{aligned} \quad (27)$$

This mapping simplifies to

$$B_j^{loc}(\xi, \eta) = \left(1 - \frac{\eta}{h}\right) \frac{\xi}{\zeta} \begin{pmatrix} 1 \\ -\tan \alpha_1 \end{pmatrix} + \frac{\eta}{h} \left(\begin{pmatrix} 0 \\ h \end{pmatrix} + \frac{\xi}{\zeta} \begin{pmatrix} 1 \\ \tan \alpha_2 \end{pmatrix} \right) \quad (28)$$

since we can set $x_1 = x_2 = 0$, $y_1 = 0$, $y_2 = h$, $\eta_1 = 0$, $\eta_2 = h$, $\beta_1 = -\alpha_1$ and $\beta_2 = \alpha_2$ without loss of generality. Using the abbreviations $a_1 = \tan \alpha_1$, $a_2 = \tan \alpha_2$ and $a = \tan \alpha_1 + \tan \alpha_2$ the Jacobian of B_j^{loc} is

$$J_j(\xi, \eta) = \begin{pmatrix} \frac{1}{\zeta} & 0 \\ -\frac{1-\eta}{\zeta} a_1 + \frac{\eta}{\zeta} a_2 & 1 + \frac{\xi}{h\zeta} a \end{pmatrix}. \quad (29)$$

With $|J_j| = (h\zeta + \xi a)/(h\zeta^2)$ we have

$$J_j^{-1}(\xi, \eta) = \begin{pmatrix} \zeta & -\frac{\zeta h(-a_1 + \eta a)}{h\zeta + a\xi} \\ 0 & \frac{\zeta h}{h\zeta + a\xi} \end{pmatrix}, F_j = \begin{pmatrix} \zeta + \frac{\xi}{h} a & a_1 - \eta a \\ a_1 - \eta a & h \frac{(a_1 - \eta a)^2 + 1}{h\zeta + \xi a} \end{pmatrix}.$$

Inserting these results in (20) yields

$$A_2^{(j)} = (h_j \zeta_j + \xi a_j) \begin{pmatrix} \frac{1}{3} & \frac{1}{6} \\ \frac{1}{6} & \frac{1}{3} \end{pmatrix} \quad (30)$$

$$A_1^{(j)} = \frac{1}{3} \begin{pmatrix} a_j & -a_{2,j} + 2a_{1,j} \\ 2a_{2,j} - a_{1,j} & a_j \end{pmatrix} \quad (31)$$

$$A_0^{(j)} = \frac{1}{3} \frac{1}{h_j \zeta_j + \xi a_j} \begin{pmatrix} -a_{1,j}^2 + a_{1,j} a_{2,j} - a_{2,j}^2 - 3 & a_{1,j}^2 - a_{1,j} a_{2,j} + a_{2,j}^2 + 3 \\ a_{1,j}^2 - a_{1,j} a_{2,j} + a_{2,j}^2 + 3 & -a_{1,j}^2 + a_{1,j} a_{2,j} - a_{2,j}^2 - 3 \end{pmatrix} \\ + (h_j \zeta_j + \xi a_j) \frac{k_j^2}{\zeta_j^2} \begin{pmatrix} \frac{1}{3} & \frac{1}{6} \\ \frac{1}{6} & \frac{1}{3} \end{pmatrix}. \quad (32)$$

If $\mathbf{u}_{s,k}^h(\xi)$ is the coefficient-vector with degrees of freedom corresponding to segment k , a local contribution to the left-hand side of (16) is

$$\sum_{j=0}^2 \left(\sum_{i=-1}^1 (h_k \zeta_k + \xi a_k)^i M_{i,j}^{(k)} \right) \partial_\xi^j \mathbf{u}_{s,k}^h(\xi) = \sum_{j=0}^2 A_j^{(k)} \partial_\xi^j \mathbf{u}_{s,k}^h \quad (33)$$

with

$$M^{(k)} \{-1, 0\} = \frac{1}{3} \begin{pmatrix} -a_1^2 + a_1 a_2 - a_2^2 - 3 & a_1^2 - a_1 a_2 + a_2^2 + 3 \\ a_1^2 - a_1 a_2 + a_2^2 + 3 & -a_1^2 + a_1 a_2 - a_2^2 - 3 \end{pmatrix}^{(k)}, \\ M^{(k)} \{1, 0\} = \frac{k_k^2}{\zeta_k^2} \begin{pmatrix} \frac{1}{3} & \frac{1}{6} \\ \frac{1}{6} & \frac{1}{3} \end{pmatrix}, \\ M^{(k)} \{0, 1\} = \frac{1}{3} \begin{pmatrix} a & -a_2 + 2a_1 \\ 2a_2 - a_1 & a \end{pmatrix}^{(k)}, \\ M^{(k)} \{1, 2\} = \frac{1}{3} \begin{pmatrix} 1 & \frac{1}{2} \\ \frac{1}{2} & 1 \end{pmatrix}, \quad (34)$$

and all other matrices $M_{ij}^{(k)} = 0$. This reveals that the entries of the globally assembled matrices $A_0(\xi)$, $A_1(\xi)$, $A_2(\xi)$ are composed of rational expressions in ξ . Due to $\zeta_k h_k > 0$ and $a_k > 0$, there is no pole for a complex ξ with $\Re(\xi) > 0$. This guarantees the presumed analyticity of the matrices.

With the complex extension of the PML-method, the left-hand side of (33)

reads

$$\sum_{j=0}^2 \left(\sum_{i=-1}^1 (h_k \zeta^k + (\gamma \xi) a_k)^i M^{(k)} \{i, j\} \right) \left(\frac{1}{\gamma} \right)^j \partial_\xi^j \mathbf{u}_{\text{PML},k}(\xi). \quad (35)$$

5 Solution of the semi-discrete PML-system by the Finite-Element-Method

We solve the ordinary differential equation (18) by a finite-element-discretization. Different numerical techniques such as spectral methods or finite differences would be possible, too.

Component m' of $\mathbf{u}_{\text{PML},k}(\xi)$ is approximated by

$$u_{\text{PML},k,m'}^h(\xi) = \sum_{n'=1}^{N_\xi} c_{\text{PML},k,m'n'} \Phi_{m'n'}(\xi), \quad (36)$$

where $\{\Phi_{m'_1}, \dots, \Phi_{m'_{N_\xi}}\}$ is a basis of the finite element space $X_h \subset C^2(\mathbb{R}_+)$. Additional degrees of freedom $n_{\text{PML},k,m'}$ are introduced on the boundary $\partial\Omega$ by

$$n_{\text{PML},k,m'} = \partial_\xi u_{\text{PML},k,m'}^h(0). \quad (37)$$

Because of the expected absorbing character of the PML-layer we impose a zero Dirichlet boundary condition on the outer boundary $\xi = \rho$. Multiplying (35) by the test function $(\Phi_{n'}^k)^*$ with components $(\Phi_{m'n'}^k)^*$ and integrating over the layer in ξ -direction yields after an integration by parts

$$\sum_{m'n'} (S_{mn,m'n'}^k + D_{mn,m'n'}^k + M_{mn,m'n'}^k) c_{\text{PML},k,m'n'} + \sum_{m'} R_{mn,m'}^k n_{\text{PML},k,m'} \quad (38)$$

with

$$S_{mn,m'n'}^k = -M_{mm'}^{(k)} \{1, 2\} \int_0^\rho \frac{1}{\gamma^2} (h_k \zeta_k + (\gamma \xi) a_k) \partial_\xi \Phi_{mn}^* \partial_\xi \Phi_{m'n'} d\xi \quad (39)$$

$$\begin{aligned} D_{mn,m'n'}^k &= -M_{mm'}^{(k)} \{1, 2\} \int_0^\rho \partial_\xi \frac{1}{\gamma^2} \partial_\xi (h_k \zeta_k + (\gamma \xi) a_k) \Phi_{mn}^* \partial_\xi \Phi_{m'n'} d\xi \\ &\quad + M_{mm'}^{(k)} \{1, 2\} \int_0^\rho \frac{1}{\gamma^2} (h_k \zeta_k + (\gamma \xi) a_k) \Phi_{mn}^* \partial_\xi \Phi_{m'n'} d\xi, \end{aligned} \quad (40)$$

$$\begin{aligned} M_{mn,m'n'}^k &= M_{mm'}^{(k)} \{-1, 0\} \int_0^\rho (h_k \zeta_k + (\gamma \xi) a_k)^{-1} \Phi_{mn}^* \Phi_{m'n'} d\xi \\ &\quad + M_{mm'}^{(k)} \{-1, 0\} \int_0^\rho (h_k \zeta_k + (\gamma \xi) a_k)^{-1} \Phi_{mn}^* \Phi_{m'n'} d\xi \end{aligned} \quad (41)$$

$$R_{mn,m'}^k = \sum_{j=0}^2 \left[\frac{1}{\gamma^2} (\gamma \xi)^j (M_{j,2})_{mm'} \Phi_{mn}^* \right]_0^\rho. \quad (42)$$

Assembling (38) to a global system yields

$$(S + D + M)\mathbf{c}_{\text{PML}} + R\mathbf{n}_{\text{PML}} = 0. \quad (43)$$

The discrete interior problem reads: Seek u^h in $V_h = \text{span}\{\varphi_1, \dots, \varphi_{N_I}\} \subset H^1(\Omega)$ such that

$$\begin{aligned} & \int_{\Omega} \nabla u^h(\mathbf{x}) \cdot \nabla \varphi_i(\mathbf{x}) \mathbf{d}\mathbf{x} - \int_{\Omega} k^2(\mathbf{x}) u^h(\mathbf{x}) \varphi_i(\mathbf{x}) \mathbf{d}\mathbf{x} - \int_{\partial\Omega} \partial_n u_s^h(\mathbf{x}) \varphi_i(\mathbf{x}) \mathbf{d}s \\ & = \int_{\partial\Omega} \partial_n u_i(\mathbf{x}) \varphi_i(\mathbf{x}) \mathbf{d}s \quad \text{for } i = 1, \dots, N_I. \end{aligned} \quad (44)$$

The coefficient vector of u^h is denoted by $\mathbf{U} = \{U_1, \dots, U_{N_I}\}$. The exterior and the interior problem couple via the boundary integral on the left-hand side of (44). Let $\pi : \{1, \dots, N\} \rightarrow \{1, \dots, N_I\}$ be a mapping from the degrees of freedom corresponding to $\partial\Omega$ to the global numbering of degrees of freedom in the discrete interior problem. A local contribution of the boundary term is

$$\begin{aligned} & \int_{p_i}^{p_j} \varphi_{\pi(i)}(s) \mathbf{n}(s) \nabla_{xy} u_{s,j}^h(s) \mathbf{d}s \\ & = h \int_0^1 \varphi_{\pi(i)}(\eta) (1, 0) J^{-T} \nabla_{\xi\eta} (u_{s,j}^h(0) \varphi_{\pi(j)}(\eta)) \mathbf{d}\eta \\ & = \underbrace{\left(h \int_0^1 \varphi_{\pi(i)}(\eta) (J^{-T})_{11} \varphi_{\pi(j)}(\eta) \mathbf{d}\eta \right)}_{(B_1)_{ij}} \partial_{\xi} u_{s,j}^h(0) \\ & \quad + \underbrace{\left(h \int_0^1 \varphi_{\pi(j)}(\eta) (J^{-T})_{12} \partial_{\eta} \varphi_{\pi(j)}(\eta) \mathbf{d}\eta \right)}_{(B_0)_{ij}} u_{s,j}^h(0), \end{aligned} \quad (45)$$

with $i, j = 1, \dots, N$, where N is the number of degrees of freedom on $\partial\Omega$. The boundary integrals can be expressed in vector notation as

$$\begin{pmatrix} \int_{\partial\Omega} \partial_n u_s^h(\mathbf{x}) \varphi_{\pi(1)}(\mathbf{x}) \mathbf{d}s \\ \vdots \\ \int_{\partial\Omega} \partial_n u_s^h(\mathbf{x}) \varphi_{\pi(N)}(\mathbf{x}) \mathbf{d}s \end{pmatrix} = B_0 \begin{pmatrix} U_{\pi(1)} \\ \vdots \\ U_{\pi(N)} \end{pmatrix} + \frac{1}{\gamma} B_1 \begin{pmatrix} n_{\text{PML},1} \\ \vdots \\ n_{\text{PML},N} \end{pmatrix}. \quad (46)$$

Let P be the matrix corresponding to the mapping $\pi(i)$, ($i = 1, \dots, N$). With

$$u^h(\mathbf{x}) = \sum_{i=1}^{N_I} U_i \varphi_i(\mathbf{x}) \quad (47)$$

the discrete interior problem reads

$$\begin{aligned}
& \sum_{j=1}^{N_I} \left(\underbrace{\int_{\Omega} \nabla \varphi_i(\mathbf{x}) \cdot \nabla \varphi_j(\mathbf{x}) dx}_{K_{ij}} - \underbrace{\int_{\Omega} k^2(\mathbf{x}) \varphi_i(\mathbf{x}) \varphi_j(\mathbf{x}) dx}_{M_{ij}} \right) U_j \\
& + \sum_{j=1}^{N_I} \sum_{k=1}^N P_{ik} \sum_{l=1}^N B_{0,kl} (P^T)_{lj} U_j + \sum_{k=1}^N P_{ik} \frac{1}{\gamma} \sum_{l=1}^N B_{1,kl} d_l \\
& = \underbrace{\int_{\partial\Omega} \partial_n u_i(\mathbf{x}) \varphi_i(\mathbf{x}) dx}_{g_i}.
\end{aligned} \tag{48}$$

The decomposition $u(\mathbf{x})|_{\partial\Omega} = u_i(\mathbf{x})|_{\partial\Omega} + u_s(\mathbf{x})|_{\partial\Omega}$ requires

$$P^T U = Q c_{\text{PML}} + U_i, \tag{49}$$

where $\tilde{c}_{\text{PML}} = Q c_{\text{PML}}$ are the degrees of freedom in c_{PML} corresponding to $\partial\Omega$ and U_i are the degrees of freedom of the incoming field on the boundary. Gathering together (43), (48) and (49) yields the global system

$$\begin{pmatrix} K + M + PB_0 P^T & 0 & \frac{1}{\gamma} P B_1 \\ 0 & S + D + M & R \\ P^T & -Q & 0 \end{pmatrix} \begin{pmatrix} U \\ c_{\text{PML}} \\ n_{\text{PML}} \end{pmatrix} = \begin{pmatrix} g \\ 0 \\ U_i \end{pmatrix}. \tag{50}$$

This system can be further simplified. In (50) the coupling conditions between the exterior and the interior problem appear explicitly. This resembles a domain decomposition approach. In the following we will show that the additional degrees of freedom on the boundary can be avoided. The resulting system (57) also arises from a finite element system based on mixed triangular and quadrilateral elements. In this case we scale the PML-equation by γ to incorporate the matching of the exterior-interior Neumann data as a natural boundary condition. Let the degrees of freedom of the PML-layer be arranged as

$$c_{\text{PML}} = \begin{pmatrix} \tilde{c}_{\text{PML}} \\ c'_{\text{PML}} \end{pmatrix}. \tag{51}$$

Accordingly we split $A := S + D + M$ as

$$A = \begin{pmatrix} A_{11} & A_{12} \\ A_{21} & A_{22} \end{pmatrix}. \tag{52}$$

We scale the PML equation with γ

$$\begin{pmatrix} K + M + PB_0P^T & 0 & \frac{1}{\gamma}PB_1 \\ 0 & \gamma \begin{bmatrix} A_{11} & A_{12} \\ A_{21} & A_{22} \end{bmatrix} & \begin{bmatrix} \gamma R \\ 0 \\ 0 \end{bmatrix} \\ P^T & -Q & 0 \end{pmatrix} \begin{pmatrix} U \\ \tilde{c}_{\text{PML}} \\ c'_{\text{PML}} \\ n_{\text{PML}} \end{pmatrix} = \begin{pmatrix} g \\ 0 \\ U_i \end{pmatrix} \quad (53)$$

and use

$$\tilde{c}_{\text{PML}} = P^T U - U_i \quad (54)$$

to obtain the equivalent system

$$\begin{pmatrix} K + M + PB_0P^T & 0 & \frac{1}{\gamma}PB_1 \\ \gamma \begin{bmatrix} A_{11}P^T \\ A_{21}P^T \end{bmatrix} & \gamma \begin{bmatrix} A_{12} \\ A_{22} \end{bmatrix} & \begin{bmatrix} \gamma R \\ 0 \end{bmatrix} \end{pmatrix} \begin{pmatrix} U \\ c'_{\text{PML}} \\ n_{\text{PML}} \end{pmatrix} = \begin{pmatrix} g \\ \gamma A_{11}U_i \\ \gamma A_{21}U_i \end{pmatrix}. \quad (55)$$

Performing elementary row operations yields

$$\begin{pmatrix} K + M + PB_0P^T + \gamma PA_{11}P^T & PA_{12} & \frac{1}{\gamma}PB_1 + P\gamma R \\ \gamma[A_{21}P^T] & \gamma[A_{22}] & [0] \\ [0] & [0] & [0] \end{pmatrix} \begin{pmatrix} U \\ c'_{\text{PML}} \\ n_{\text{PML}} \end{pmatrix} \quad (56)$$

$$= \begin{pmatrix} g + \gamma PA_{11}U_i \\ \gamma A_{21}U_i \\ 0 \end{pmatrix}.$$

Since $\frac{1}{\gamma}PB_1 + P\gamma R = 0$, according to (42) and (46) we obtain the equivalent reduced system

$$\begin{pmatrix} K + M + PB_0P^T + \gamma PA_{11}P^T & PA_{12} \\ \gamma[A_{21}P^T] & \gamma[A_{22}] \end{pmatrix} \begin{pmatrix} U \\ c'_{\text{PML}} \end{pmatrix} = \begin{pmatrix} g + \gamma PA_{11}U_i \\ \gamma A_{21}U_i \end{pmatrix}. \quad (57)$$

6 Numerical examples

The scattering problem (3)-(6) is solved for two different examples with known exact solution in order to investigate the convergence of the computed solution in dependence of the thickness ρ of the PML layer. In general it is a difficult

task to verify the expected exponential convergence behavior in a numerical experiment. Since the finite element method converges only polynomially, the discretization error asymptotically dominates the error caused by the finite thickness of the PML-layer. We therefore carry out a special discrete convergence check for the quality of the transparent boundary condition. We solve a sequence of discrete problems with fixed interior triangulation and a discretization in the PML-layer given by $\xi = [0 : h_{\text{PML}} : jh_{\text{PML}}]$. Here h_{PML} is the mesh width in ξ -direction and jh_{PML} is the thickness of the PML-layer. Then we expect that the computed solution $u_{h,j}$ of the interior domain converges exponentially to $u_{h,\infty}$ for $j \rightarrow \infty$. We repeat this experiment for a halved mesh width in the interior domain together with the refinement $h_{\text{PML}} := h_{\text{PML}}/2$.

In the first experiment we solve a waveguide scattering problem for the case of TM-polarization with geometry as depicted in Fig. 9. On the left end of the waveguide an incoming wave is given as an eigenmode of the waveguide. The electric field is computed in the inner domain $[-10, 10] \times [-10, 10]$ with linear and quadratic finite elements (128249 degrees of freedom). The thickness of the PML-layer varies from $\rho = 0.2$ to $\rho = 5.6$. The layer is discretized with 4 points per 0.2 respectively 0.4 length units in ξ -direction (linear respectively quadratic elements). Fig. 10 shows a semilog plot of the relative error $e_1 := \|u - u_h\|_2 / \|u\|_2$ in dependence of the thickness ρ of the PML-layer. For a

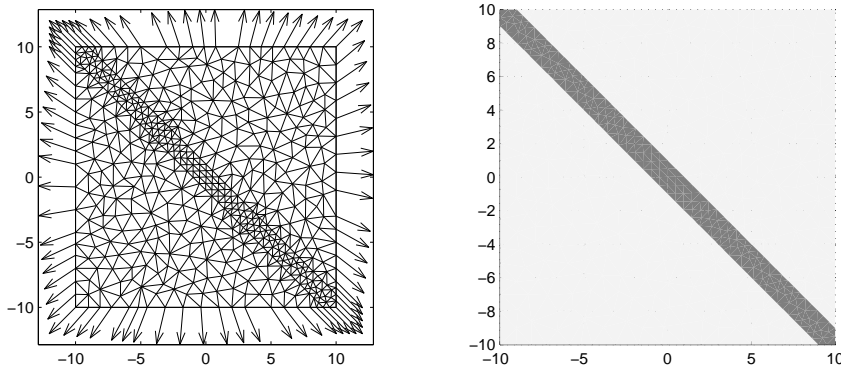


Fig. 9. Discretization of the interior domain and rays in the exterior domain (left picture). Geometry with representation of the refractive index distribution (right picture). Infinite waveguide: $n = 6.6$, background: $n = 1.45$.

small thickness of the PML-layer and a huge number of degrees of freedom in the finite element discretization the error caused by the finite thickness of the PML-layer dominates. Here the error e_1 shows an exponential convergence behavior in dependence of ρ . With growing thickness of the PML-layer the discretization error becomes more and more relevant. From $\rho = 2.5$ for linear elements and $\rho = 5$ for quadratic elements a further increase of ρ has no influence on the error.

Fig. 11 shows a semilog plot of the sequence $e_2(j) = \|u_{h,J} - u_{h,j}\|_2 / \|u_{h,J}\|_2$ in

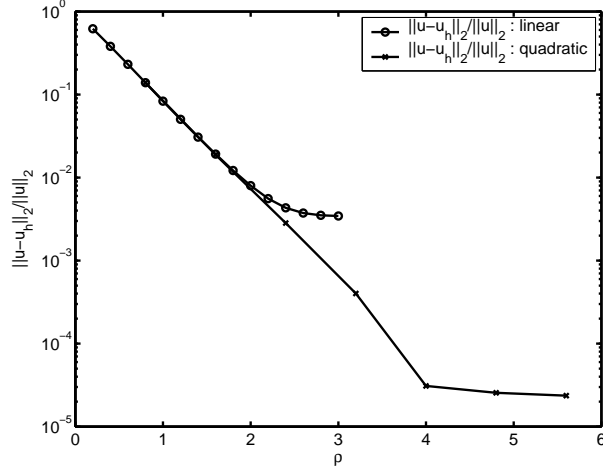


Fig. 10. Relative error $\|u - u_h\|_2 / \|u\|_2$ versus thickness of the PML-layer for linear and quadratic finite elements in the first experiment.

dependence of the thickness of the PML-layer $\rho = j h_{PML}$. We replace $u_{h,\infty}$ by $u_{h,J}$ with $J := 10/h_{PML}$. The sequence converges exponentially in dependence of ρ , with two different rates. The smaller absolute value of the rate appears in the range of ρ where the discretization error dominates and the error caused by the finite thickness of the PML-layer is negligible. The left part of the graph approaches the error $e_2 = \|u^* - u(\rho)\|_2 / \|u^*\|_2$ with $u^* = \lim_{\rho \rightarrow \infty} u(\rho)$ for an increasing number of degrees of freedom.

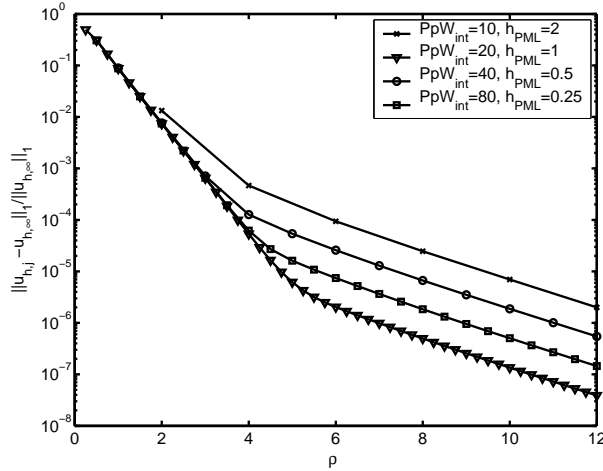


Fig. 11. Relative error $e_2(j) = \|u_{h,j} - u_{h,\infty}\|_2 / \|u_{h,\infty}\|_2$ for different numbers of degrees of freedom in the linear finite element discretization (increasing from top to down) in the first experiment.

In the second experiment we solve a cylinder scattering problem for the case of TM-polarization, with zero boundary condition for the electric field. The geometry is depicted in Fig. 12. The electric field is computed in the inner domain $[-10, 10] \times [-10, 10] \setminus B(0, 1)$ with linear and quadratic finite elements

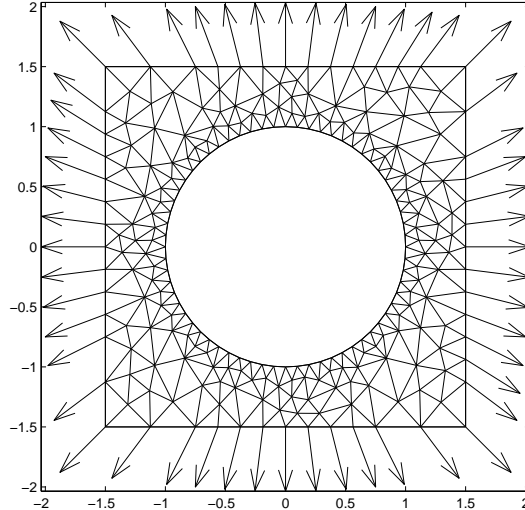


Fig. 12. Discretization of the interior domain and rays in the exterior domain.

(153076 degrees of freedom). The thickness of the PML-layer varies from $\rho = 0.2$ to $\rho = 10.0$. The layer is discretized with 4 points per 1.0 respectively 0.8 length units in ξ -direction (linear respectively quadratic elements). Fig. 13 shows a semilog plot of the relative error $e_1 := \|u - u_h\|_2 / \|u\|_2$ in dependence of the thickness ρ of the PML-layer. Again there is exponential convergence of the error e_1 with ρ in the range where the error caused by the finite thickness of the PML-layer dominates. This time quadratic finite elements lead to a better rate in the semilog plot.

Fig. 14 shows a semilog plot of the sequence $e_2(j) = \|u_{h,*} - u_{h,j}\|_2$ in dependence of the thickness of the PML-layer $\rho = jh_{PML}$. Again we replace $u_{h,\infty}$ by $u_{h,J}$ with $J := 10/h_{PML}$. The sequence shows the same exponential convergence behavior as in the first experiment.

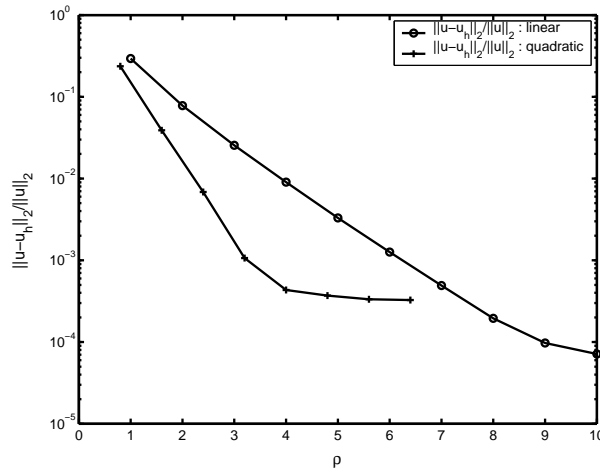


Fig. 13. Relative error $\|u - u_h\|_2 / \|u\|_2$ versus thickness of the PML-layer for linear and quadratic finite elements in the second experiment.

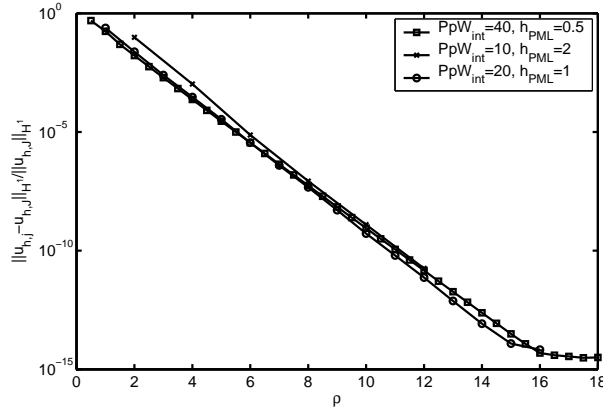


Fig. 14. Relative error $e_2(j) = \|u_{h,J} - u_{h,j}\|_2 / \|u_h(\infty)\|_2$ for different numbers of degrees of freedom in the linear finite element discretization (increasing from top to down, determined by the points per wavelength (PpW)) in the second experiment.

7 Conclusions

The PML-method has been formulated in the context of F. Schmidt's discretization scheme of the exterior domain [12]. This provides a tool for solving scattering problems with inhomogeneous exterior domains in the case, where the refraction index distribution allows to choose a decomposition in segments with constant refractive index. Numerical experiments have indicated exponential convergence of the error $\|u - u(\rho)\|_2$ in dependence of the thickness ρ of the PML-layer.

References

- [1] J. Berenger, A perfectly matched layer for the absorption of electromagnetic waves., *J. Comput. Phys.*, 1994, 114, 2, pp. 185-200,
- [2] W.C. Chew and J.M. Jin and E. Michielssen, Complex Coordinate Stretching as a Generalized Absorbing Boundary Condition, unpublished
- [3] W.C. Chew and W.H. Weedon, A 3-D Perfectly Matched Medium from Modified Maxwell's Equations with Stretched Coordinates, *Micro. Opt. Tech. Lett.*, 7 (13) 1994
- [4] W.C. Chew and W.H. Weedon, A 3-D Perfectly Matched Medium by Coordinate Stretching and Its Absorption of Static Fields, *Applied Computational Electromagnetics Symposium Digest*, pp. 482-489, 1995, 1
- [5] F. Collino and P. Monk, The perfectly matched layer in curvilinear coordinates, *SIAM J. Sci. Comput.*, 1998, 19, 6, pp. 2061-2090

- [6] T. Hohage and F. Schmidt and L. Zschiedrich, Solving time-harmonic scattering problems based on the pole condition: Theory, Zuse Institut Berlin (ZIB), 2001, *Preprint 01-01*
- [7] T. Hohage and F. Schmidt and L. Zschiedrich, Solving time-harmonic scattering problems based on the pole condition: Convergence of the PML-method, Konrad-Zuse-Zentrum (ZIB), 2001, *Preprint 01-23*
- [8] F. Ihlenburg, Finite Element Analysis of Acoustic Scattering, *Springer*, 1998
- [9] M. Lassas and J. Liukkonen and E. Somersalo, Complex Riemannian metric and absorbing boundary condition., *J. Math. Pures Appl.* 2001, 80, 7, pp. 739–768
- [10] M. Lassas and E. Somersalo, On the existence and convergence of the solution of PML equations., *Computing No.3, 229-241*, 1998, 60, 3, pp. 229-241
- [11] M. Lassas and E. Somersalo, Analysis of the PML equations in general convex geometry, *Proc. Roy. Soc. Edinburgh Sect. A 131*, pp. 1183–1207, 2001
- [12] F. Schmidt, A New Approach to Coupled Interior-Exterior Helmholtz-Type Problems: Theory and Algorithms, Konrad-Zuse-Zentrum Berlin, Fachbereich Mathematik und Informatik, FU Berlin, 2001, *Habilitation thesis*
- [13] H. Shaker, Ein neues Verfahren zur Lösung des Streuproblems der Maxwell-Gleichungen, Universität Hamburg, Fachbereich Physik. Diplomarbeit
- [14] W. Walter, Gewöhnliche Differentialgleichungen, Springer Verlag, 1993.